

This article appeared in a journal published by Elsevier. The attached copy is furnished to the author for internal non-commercial research and education use, including for instruction at the authors institution and sharing with colleagues.

Other uses, including reproduction and distribution, or selling or licensing copies, or posting to personal, institutional or third party websites are prohibited.

In most cases authors are permitted to post their version of the article (e.g. in Word or Tex form) to their personal website or institutional repository. Authors requiring further information regarding Elsevier's archiving and manuscript policies are encouraged to visit:

<http://www.elsevier.com/copyright>



Metal-Enhanced Fluorescence (MEF): Physical characterization of Silver-island films and exploring sample geometries

R. Pribik^a, A.I. Dragan^a, Y. Zhang^a, C. Gaydos^b, C.D. Geddes^{a,*}

^aInstitute of Fluorescence, University of Maryland Biotechnology Institute, 701 East Pratt Street, MD 21202, USA

^bJohn Hopkins University, 855 North Wolfe St, 530 Rangos, Baltimore, MD 21205, USA

ARTICLE INFO

Article history:

Received 5 May 2009

In final form 8 July 2009

Available online 12 July 2009

ABSTRACT

In this study we have analyzed metal-enhanced fluorescence (MEF) effects from different density Silver-island films (SiFs) and the effects of sample geometry on the observed enhancement of fluorescence (EF). It is shown that silver islands grow exponentially with SiF deposition time ($DT < 5$ min), optical density of SiFs almost linearly depends on DT; electrical conductivity is zero. At $DT > 5$ min, silver islands merge, exhibiting a sharp increase in electrical conductivity. It has been shown that the newly proposed SiF sample geometry exhibits higher EF values than the commonly used in MEF studies SiF–SiF sample geometry. The SiF–glass geometry demonstrates high sensitivity for surface immunoassays, a growing application of metal-enhanced fluorescence.

© 2009 Elsevier B.V. All rights reserved.

1. Introduction

Fluorescence spectroscopy has changed significantly in recent years due to the discovery of metal-enhanced fluorescence (MEF), a metal–fluorophore interaction that greatly increases the observed emission intensity [2,14,15,20,21]. Since the discovery of MEF the phenomenon has been applied to several bio-assays [1,2,9]. Furthermore, many studies of MEF have been conducted and the results were obtained using a sample geometry where two metal-deposited slides are sandwiched together with the fluorescent sample within. The study here shows that the enhancement factors measured in this geometry are to an extent erroneous. Thus we propose a different sample geometry that more accurately measures the magnitude of fluorescence enhancement, as well as more closely represents the sample geometry used in bio-assay applications of MEF, a growing application.

Several metals have been shown to be useful in MEF, such as silver, gold, copper, aluminum, nickel, zinc, and most recently chromium [3,6,8,10,11,17]. Silver is perhaps the most commonly used metal in MEF as it exhibits strong plasmon resonance around 420 nm, and due to the relative simplicity of Silver-island Films (SiFs) preparation in the laboratory.

When preparing SiFs, the size of the silver nanoparticles, and therefore the thickness of the deposition can be loosely controlled by the time allowed for the deposition to occur. We begin this study by physically characterizing SiFs of various deposition times from 1 to 8 min by atomic force microscopy, optical density, and

conductivity. Finally, SiFs made using the same process are then used in a comparison of two different sample geometries, SiF–SiF and SiF–glass, where a fluorophore solution is sandwiched between two SiFs, or one SiF and a blank glass side, respectively. It is found that the SiF–glass geometry improves enhancement measurements for all deposition times, which in terms of MEF applications, suggests better surfaces for immunoassays.

2. Experimental

- 1. Materials.** Fluorophores and materials including fluorescein (salt), fluorescein isothiocyanate, Nile Blue, Rhodamine B, Rose Bengal, silane-prep™ glass microscope slides, and solid silver nitrate were purchased from Sigma–Aldrich Chemical Company (Milwaukee, WI, USA).
- 2. Preparation of Silver-island films.** Silver-island films were prepared according to the procedure found in Ref. [13]. Deviations in SiF thickness were reduced by using a fresh selection of silane-prep™ slides. The fabricated samples and process were highly reproducible, which gave an opportunity for careful characterization of the physical properties of the SiF samples. The slides were stored in a vacuum between SiF preparations to reduce oxidation.
- 3. Preparation of sandwich geometries for metal-enhanced fluorescence measurements.** A solution of 150 μ L of fluorophore (<500 μ M) was sandwiched between two glass slides for the glass control measurements, one glass and one SiF slide for the SiF–glass geometry measurements, and two SiF slides for the SiF–SiF geometry measurements. This was undertaken for

* Corresponding author. Fax: +1 410 576 5722.

E-mail address: geddes@umbi.umd.edu (C.D. Geddes).

all the deposition times, and a new control was used for each set of data. The first pair of slides was removed from the silver depositing solution after 1 min, then the second pair was removed after 2 min, and so on for up to 8 min depositions, where the solution silver capacity far-exceeded the capacity to coat the slides.

4. *Optical spectroscopy.* The emission spectra of fluorophores were recorded with an Ocean Optics HD2000 fluorometer, and the absorption spectra of the dry SiF slides were measured with a Varian Cary 50 UV–vis spectrophotometer. Six intensity measurements were averaged for each enhancement factor calculation, where each of the measurements was taken randomly across the surface of the sample. Solid-state lasers centered at 473, 532, and 593 nm were used, as the excitation sources. It was noted that the emission intensity decreased as the detector was moved from top to bottom of the slide. Each slide was measured twice at the top of the deposition region, twice in the middle region, and twice toward the bottom region.

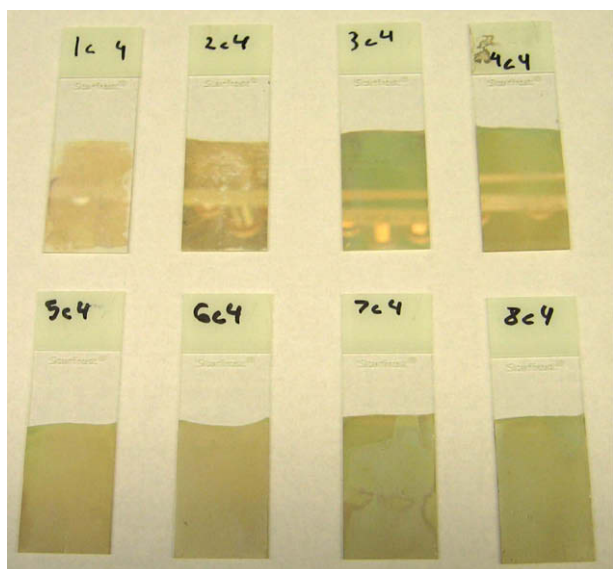


Fig. 1. Real color photographs of silver island films deposited on glass slides at deposition times ranging from 1 to 8 min, in 1-min increments, from left to right, top to bottom.

5. *Atomic force microscopy (AFM).* AFM images were collected on a Molecular Imaging Picoplus Microscope. Samples were imaged at a scan rate of 1 Hz with 512×512 pixel resolution in contact mode.
6. *Electrical conductivity.* Conductivity of SiFs was measured with a Exttech 382213 DC regulated power supply. A constant voltage was applied across a 1 cm distance between contacts on the SiF slide. Resistance and voltage were recorded to determine conductivity values.

3. Results

By changing the amount of time that the glass slide is submerged in the silver deposition solution it is possible to make SiFs of varying thickness (Fig. 1). Through the use of atomic force microscopy, absorption spectroscopy, and electrical conductivity, it is possible to quantify the size and dimensions of the silver islands for different deposition times, determine a relative relationship of Silver-island size to deposition time and optical density, and determine the continuity of the metal on the glass surface, respectively.

The first method of SiF quantification is through the use of atomic force microscopy (AFM), as can be seen in Fig. 2. A set of AFM images show that an increase of silver deposition time (DT) from 1 to 7 min increases the size of the silver islands, their density on a glass surface and an average inter-particle distance. Diameter of the particles changes from 10–30 Å (deposition time of 1 min) to about 300 nm at the deposition time of 7 min. The images, shown in Fig. 2 show that the size of the silver islands increases non-linearly, rather exponentially with the time of silver deposition. This can be explained by properties of the silver deposition technique; in particular, different adhesion of silver to a glass surface and to preformed silver islands (seeds on a surface). As a consequence wet deposition of silver onto a glass slide proceeds in two phases: formation of silver-seeds on a glass surface and time-dependent deposition of silver on preformed seeds [4], i.e. silver islands growing.

Though the optical density (OD) measured via absorption spectroscopy does not give an absolute size of the metal nanoparticles, it is a means to determine the relative amount of a metal-deposited onto a slide. Fig. 3a shows log-normal dependence of the optical density change upon the time of silver deposition. The observed changes in OD correlate with the AFM data. At short deposition

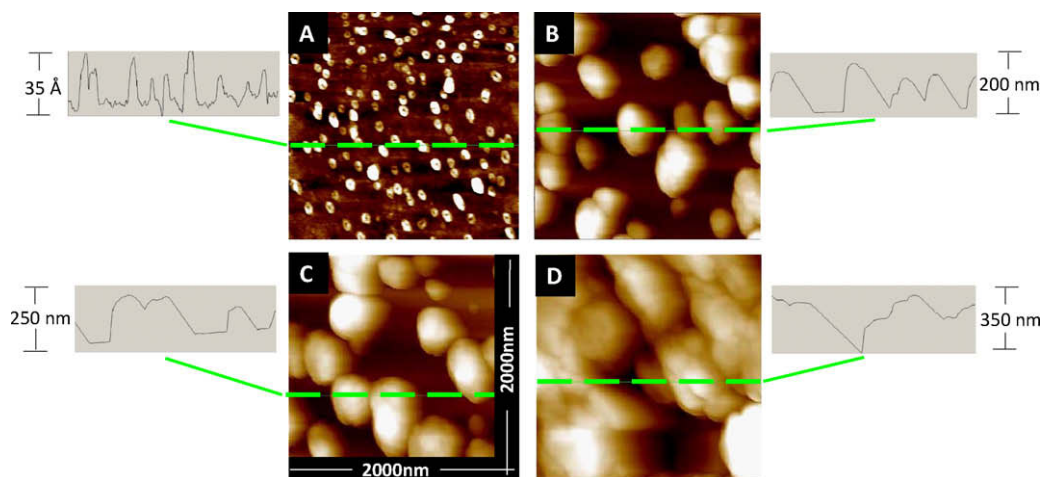


Fig. 2. AFM images for SiFs of 1, 2, 3, and 7 min (A–D, respectively) deposition times. All images are on a 2000 nm^2 scale and the scale for each cross sectional height is shown to the side of each image.

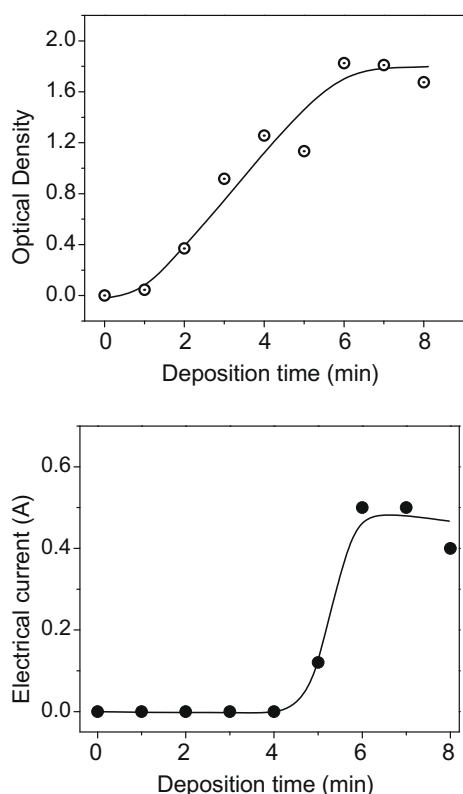


Fig. 3. The dependences of the optical density (Top) of SiFs and electrical current through silver films (Bottom) upon deposition time of silver on glass supports.

times the slope of SiFs absorption versus DT is small, which reflects the slow rate of formation of silver-seeds on a glass surface due to the low affinity of silver to the glass surface. Then, at DT > 2 min,

one can observe sharp increase in the OD values caused by the fast growing of silver islands. Interesting, at longer DT (6–8 min) the rate of the OD increase slows down. Indeed the rate of silver deposition appears to depend not only upon DT, but also the surface area accessible for silver deposition. At a certain stage of SiFs growing, inter-island distances decrease and silver islands merge, stick to each other, and the film becomes continuous. As a result, the metal surface area, exposed to solution, dramatically decreases, which leads to a decrease of the rate of silver deposition which slows down changes in optical density.

By measuring conductivity (or resistance) it is also possible to determine if the metal-deposition has reached a point of continuity. The relationship of conductivity as a function of deposition time is of interest because the sharp increase in conductivity correlates to the crossing point from discontinuous to a continuous metal surface, i.e. resistance drops to $\approx 0 \Omega$ for DTs with continuous metal surfaces. Silver films deposited at DT < 5 min exhibit zero conductivity which reflects existence of a discontinuous surface formed by separate metal islands. At DT > 5 min the conductivity of slides sharply increases reaching a plateau, i.e. zero electrical resistance. The observed changes in electrical properties correlate with optical density and AFM analysis of the SiFs surface. It should be noted that at the point of transition from discontinuous to a continuous film, when silver islands merge, we would expect to see a drop in fluorescence enhancement from the surface, as has been reported recently for just-continuous thin films [7].

Emission of fluorescein in water was measured for both geometries as shown in Fig. 4 (bottom) as well as for the glass–glass control sample. Greater emission intensities, and therefore enhancement factors, were measured for the SiF–glass arrangement for all SiF deposition times as shown in Fig. 4 (top). Furthermore, we see that the greatest emission intensity was measured for SiF deposition times of 5–7 min. In comparison the emission intensity for the SiF–SiF geometry at these deposition times is much lower.

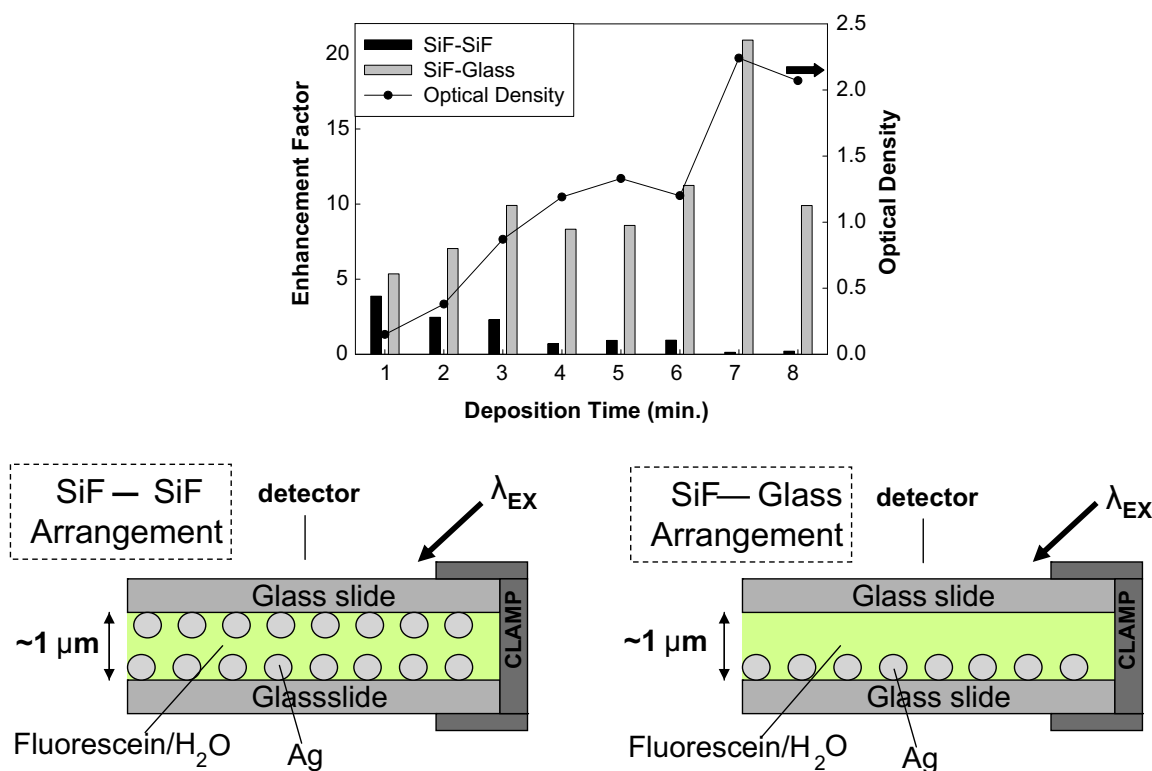


Fig. 4. The enhancement factor of fluorescein in water as a function of SiF deposition time for two different experimental arrangements (bottom). The traditional SiF–SiF arrangement yields lower enhancement factors for all deposition times.

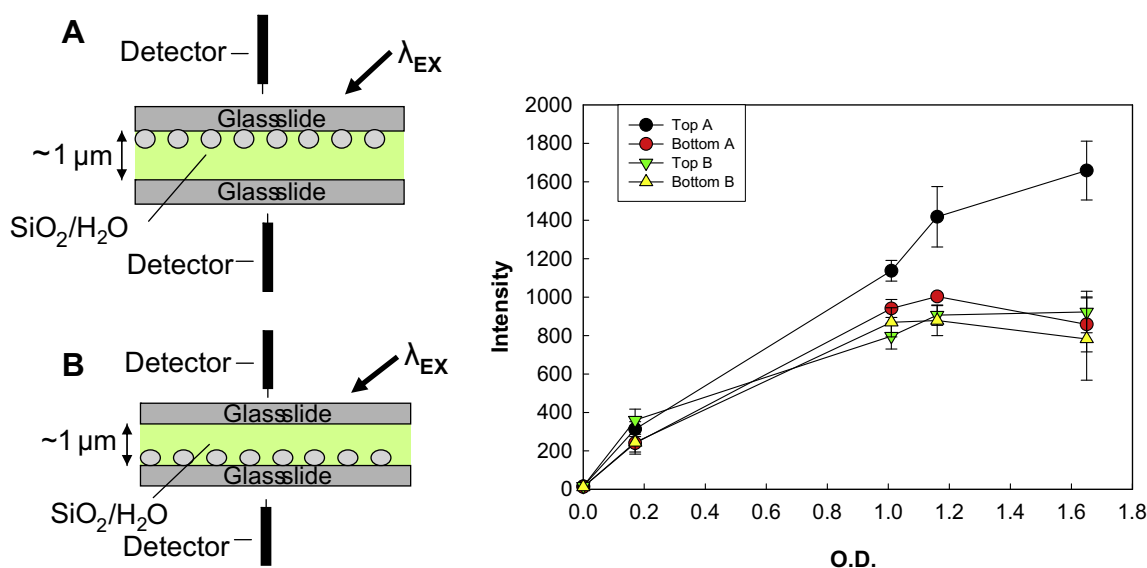


Fig. 5. SiO₂ (a scattering agent) in water is used to scatter excitation light in these two geometries and the scattered light is measured by detectors placed above and below the sample. As silver deposition thickness increases the amount of light backscattered from the top metal slide (Top A) increases.

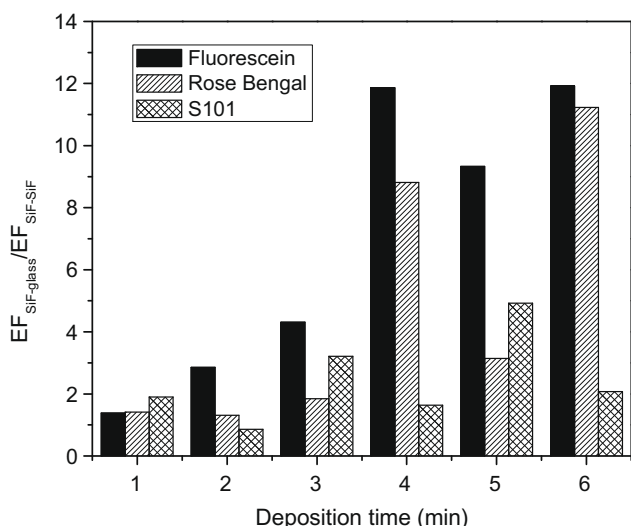


Fig. 6. The ratio of SiF-glass enhancement factor to SiF-SiF enhancement factor as a function of deposition time is shown for Fluorescein, Sulforhodamine 101 (S101), and Rose Bengal. An increase in enhancement factor is generally observed for the SiF-glass geometry.

One logical explanation for this observation is that in the SiF-SiF geometry, the excitation light is back-reflected from the silver, thus never reaching the fluorophore solution. Fig. 5 depicts the experimental geometry that was used to study this effect. Interestingly, the divergence of the 'Top A' and 'Bottom A' curves strongly supports this hypothesis, as the amount of scattered light from an SiO₂ scattering solution detected at the top detector increases as a function of deposition time, while the light detected at the bottom detector decreases.

To compare sample geometries further for other fluorophores with different maximum excitation wavelengths and quantum yields, we measured Rose Bengal ($Q_0 = 0.1$) and Sulforhodamine 101 ($Q_0 = 0.9$) at excitation wavelengths of 532 nm and 593 nm, respectively, Fig. 6.

Interestingly, by comparing the enhancement factor from the SiF-SiF geometry versus a SiF-glass geometry, a much larger

enhancement from the SiF-glass geometry can be observed. It is therefore likely that the enhancement values reported by others elsewhere [15,16,18,19] are in fact an underestimate of the possible values achievable due to the SiF-SiF geometry used.

Finally, it is also worth commenting on the value of the EF in these sample geometries. As shown in Fig. 4, the solution path length is approximately 1 μm . However, with a MEF interaction distance of <20 nm [12,13], then less than 2% of the total solution is within the enhancement region for a SiF-glass geometry (4% for a SiF-SiF geometry). This implies that the near-field enhancement factor values are approximately 50 and 25 times greater for both SiF-glass and SiF-SiF geometries, respectively. This also supports the notion that the SiF-glass geometry is much better a surface and geometry for enhancing fluorescence as depicted in Fig. 6.

4. Conclusions

The commonly used SiF-SiF sample geometry in MEF measurements has been shown to result in fluorescence enhancement values that are lower than those obtained in the newly proposed SiF-glass sample geometry. In the SiF-glass geometry, deposition times of 5 to 7 min give the greatest fluorescence enhancement. This overall net increase of enhancement factor occurs for several fluorophores including Fluorescein, Sulforhodamine 101, and Rose Bengal. The SiF-glass geometry is also a closer model to that used in MEF Bio-assays [2,3,5,12], suggesting better sensitivity of these bio-assays. Work is currently underway in our laboratory to apply these sample geometries and SiF coatings to Bio-assays.

Acknowledgements

The authors would like to thank the NIH/NIBIB 1U54EB007958-1 for financial support. The authors also thank UMBI and the IoF for salary support.

References

- [1] K. Aslan, *Analyst* 133 (2008) (1469).
- [2] K. Aslan, I. Gryczynski, J. Malicka, E. Matveeva, J.R. Lakowicz, C.D. Geddes, *Curr. Opin. Biotechnol.* 16 (2005) 55.
- [3] K. Aslan, P. Holley, C.D. Geddes, *J. Immunol. Meth.* 312 (2006) 137.
- [4] K. Aslan, Z. Leonenko, J.R. Lakowicz, C.D. Geddes, *J. Phys. Chem. B* 109 (2005) 3157.

- [5] K. Aslan, S.N. Malyn, G. Bector, C.D. Geddes, *Analyst* 132 (2007) 1122.
- [6] K. Aslan, S.N. Malyn, C.D. Geddes, *J. Fluoresc.* 17 (2007) 7.
- [7] K. Aslan, S.N. Malyn, Y.X. Zhang, C.D. Geddes, *J. Appl. Phys.* 103 (2008) 084307.
- [8] K. Aslan, K. McDonald, M.J.R. Previte, Y.X. Zhang, C.D. Geddes, *Chem. Phys. Lett.* 464 (2008) 216.
- [9] K. Aslan, M.J. Previte, Y. Zhang, T. Gallagher, L. Baillie, C.D. Geddes, *Anal. Chem.* 80 (2008) 4125.
- [10] K. Aslan, M.J.R. Previte, Y.X. Zhang, C.D. Geddes, *J. Phys. Chem. C* 112 (2008) 18368.
- [11] C.D. Geddes, H. Cao, J.R. Lakowicz, *Spectrochim. Acta A: Mol. Biomol. Spectrosc.* 59 (2003) 2611.
- [12] C.D. Geddes, I. Gryczynski, J. Malicka, Z. Gryczynski, J.R. Lakowicz, *Comb. Chem. High Throughput. Screen.* 6 (2003) 109.
- [13] C.D. Geddes, J.R. Lakowicz, *J. Fluoresc.* 12 (2002) 121.
- [14] C.D. Geddes, A. Parfenov, J.R. Lakowicz, *Appl. Spectrosc.* 57 (2003) 526.
- [15] J.R. Lakowicz et al., *J. Fluoresc.* 14 (2004) 425.
- [16] S. Mackowski et al., *Nano. Lett.* 8 (2008) 558.
- [17] R. Pribik, K. Aslan, Y.X. Zhang, C.D. Geddes, *J. Phys. Chem. C* 112 (2008) 17969.
- [18] K. Ray, R. Badugu, J.R. Lakowicz, *J. Phys. Chem. C: Nanomater. Interf.* 111 (2007) 7091.
- [19] C.R. Sabanayagam, J.R. Lakowicz, *Nucleic Acids Res.* 35 (2007) e13.
- [20] Y. Zhang, K. Aslan, M.J. Previte, C.D. Geddes, *J. Fluoresc.* 17 (2007) 627.
- [21] Y. Zhang, K. Aslan, M.J. Previte, C.D. Geddes, *Appl. Phys. Lett.* 92 (2008) 13905.